

Ion-atom two-qubit quantum gate based on phonon blockade

Subhra Mudli and Bimalendu Deb*

*School of Physical Sciences, Indian Association for the
Cultivation of Science, Jadavpur, Kolkata 700032, India.*

arXiv:2602.19222v1 [quant-ph] 22 Feb 2026

Abstract

In a previous paper [S. Mudli *et al.* Phys. Rev. A 110, 062618 (2024)], it was shown that a trapped ion can mediate interaction between two largely separated Rydberg atoms, and this mediated interaction can be leveraged to perform a universal two-qubit gate operation between neutral atom qubits in optical tweezers. In this paper, we demonstrate the universal two-qubit CNOT gate with high fidelity between an ionic and an atomic qubit relying on Rydberg excitation of the atom and the resulting phonon blockade in the motional states of the harmonically trapped ion. The phonon blockade arises due to strong ion-atom interaction when the atom is excited to a Rydberg state. These demonstrations suggest that an ion-atom hybrid system can serve as a resourceful platform or module for quantum computing and quantum networking as it can utilize the best features of charged as well as neutral atom qubits.

I. INTRODUCTION

Hybrid quantum systems that combine distinct physical platforms provide new exploratory frameworks for quantum information processing, quantum simulation and many other tasks in quantum domain. Among quantum computing platforms, superconducting circuit QED [1–4], trapped ions [5–8] and neutral atoms [9–14] are the forerunners as they have long qubit coherence times and allow precise control over their quantum states. Trapped ions are employed to create high-fidelity laser-driven quantum gates mediated by their quantized motional modes. Neutral atoms when excited to Rydberg states undergo strong long-range dipole-dipole (dd) or van der Waal (vdW) interactions that can be engineered on a fast time scale using well-designed laser pulses [15–23]. A combination of these two systems [24–27] opens the possibility of realizing hybrid quantum gates and quantum networking with an enlarged and flexible parameter domain.

When a Rydberg atom is placed close to an ion, it results in a long-range ion-atom polarization interaction that modifies the trapping potential of the ion. This interaction leads to shifts in both the equilibrium position and the vibrational frequency of the ion’s harmonic confinement. Since trapped ion quantum logic relies critically on the resonance condition between internal electronic transitions and quantized motional sidebands, such interaction-induced shifts can strongly affect the ion-phonon coupling.

Our ion-atom two-qubit gate protocol is schematically shown in Fig 1. In this proposed model,

* msbd@iacs.res.in

a single neutral atom is trapped in an optical tweezer positioned near a trapped ion in a Paul trap. It is possible to insert an optical tweezer inside the ion trap as demonstrated experimentally recently [28]. We do not want the optical tweezer to be too close to the equilibrium position to avoid direct atom-ion collision. The atomic qubit is encoded in two hyperfine ground states while an auxiliary Rydberg state of the atom is used to mediate conditional dynamics. The ionic qubit is encoded in two internal states and coupled to its quantized motional states via laser-driven sideband transitions. When the atom is excited to a Rydberg state, the ion-atom potential shifts the ion trap’s equilibrium position and frequency. This frequency shift detunes the red-sideband transition suppressing phonon exchange when the detuning exceeds the ion-phonon coupling. We call this suppression effect as phonon blockade. By exploiting this conditional phonon blockade, we design a controlled-NOT (CNOT) gate in which the atomic qubit acts as the control and ionic qubit as the target. The gate is implemented through a sequence of laser pulses. The atomic qubit is first conditionally excited to a Rydberg state followed by a sideband pulse on the ion. The transition between the ionic qubit states is either allowed or blocked depending on the qubit state of the atom.

We develop a detailed theoretical model [27] of the atom-ion system including ion-phonon coupling, laser driven internal dynamics, and the Rydberg mediated atom-ion interaction. By deriving an effective Hamiltonian in Lamb-Dicke regime, we identify the parameter conditions under which phonon blockade occurs and unwanted transitions are suppressed. Our numerical analysis using $^{87}\text{Rb}-^9\text{Be}^+$ hybrid system with realistic parameters show that an ion-atom two-qubit gate with more than 89% fidelity can be realized within a time scale that is much shorter than the lifetime of the Rydberg state. This work shows phonon blockade as a resource for quantum logic in a hybrid atom-ion platform, highlighting the importance of atomic Rydberg state-mediated ion-atom interactions, apart from ion-mediated atom-atom interactions [27] for quantum computing.

The paper is organized in the following way. In Sec II we present the model and formulate the problem. In Sec III we show numerical results and interpret them. We conclude in Sec IV.

II. THE MODEL AND FORMULATION OF THE PROBLEM

A schematic diagram of our proposed model is shown in Fig.1. An atom is trapped in an optical tweezer whose center is placed at a distance x_0 from the center of a Paul trap containing a single ion. The origin of the coordinate system is set at the electric potential minimum of the ion-trap or

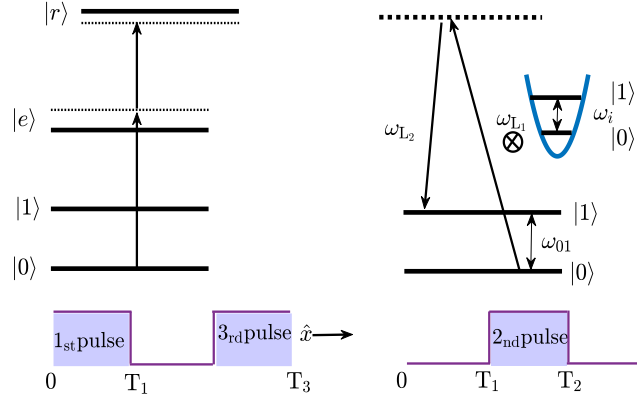


FIG. 1. A schematic of control-NOT gate using phonon blockade: A single atomic qubit (the left level diagram) is placed at a small separation from an ionic qubit (the right level diagram). The atom is assumed to be trapped in an optical tweezer which is positioned near the ion in a Paul trap. Two hyperfine levels in the ground state manifold constitute the two atomic qubit states $|0\rangle$ and $|1\rangle$. The ionic qubit may be composed of two ground-state hyperfine levels or one ground-state hyperfine level and one metastable excited level. The tweezer is considered to be collinear with the x -axis of the Paul trap. Here controlled NOT gate is realized via phonon blockade through controllable ion-atom interaction. When the atomic qubit state $|0\rangle$ is coupled to the Rydberg state $|r\rangle$ by a two-photon process via the intermediate state $|e\rangle$, the ion-atom interaction is enhanced by many orders of magnitude. Ion's qubit states are coupled to its phonon states by a two-photon laser coupling, with ω_{L_1} and ω_{L_2} being the frequencies of the two lasers. First, a two-photon π pulse acts on the control (atom), then a π rotation is given to the target (ion), lastly another π pulse is applied on the control. By this pulse sequence, a controlled NOT gate is realized (see text).

the equilibrium position of the ion.

To begin with, let us consider that the atom has the internal (electronic) states $|0\rangle_a \equiv (1 \ 0)^T$, $|1\rangle_a \equiv (0 \ 1)^T$ and $|r\rangle_a$; where $|0\rangle_a$ and $|1\rangle_a$ denote two ground-state hyperfine levels and $|r\rangle_a$ a Rydberg state. The atomic qubit is composed of $|0\rangle_a$ and $|1\rangle_a$. $|r\rangle_a$ will be employed as an auxiliary state for performing two-qubit quantum gate operations. The ionic qubit consists of $|0\rangle_i$ and $|1\rangle_i$, which may be two grounded hyperfine levels or a ground hyperfine state and a metastable excited state.

For simplicity of calculations, we consider an effective one-dimensional (1D) model system

along the x -direction, assuming the harmonic trapping frequencies of both the ion trap and the optical tweezer along y and z directions are much higher than that along x direction and both the ion and the atom are cooled to the motional ground states of harmonic oscillations along y and z direction. The ion-atom interaction Hamiltonian is $\hat{V}_{\text{ia}}(x_a, x_i) = \hat{V}_{\text{ia}}(|x_a - x_i|)$ where

$$\hat{V}_{\text{ia}} = V|r\rangle_a\langle r| \otimes |i\rangle\langle i| \quad (1)$$

Here $V = \frac{C_4}{|x_a - x_i|^4}$ with C_4 being the long-range coefficient of interaction between the ion and the atom in the Rydberg state. Since $|x_a| \gg |x_i|$, we have

$$V \simeq \frac{C_4}{x_a^4} \left[1 + \frac{4x_i}{x_a} + \frac{4x_i^2}{x_a^2} \right] = V^{(0)} + \hat{U}_1 + \hat{U}_2 \quad (2)$$

where $V^{(0)} = C_4/x_a^4$ and

$$\hat{U}_1 = U_1^{(0)} \frac{1}{\sqrt{2}} \left[a_i e^{-i\omega_i t} + a_i^\dagger e^{i\omega_i t} \right] \quad (3)$$

$$\hat{U}_2 = U_2^{(0)} \left[a_i^2 e^{-2i\omega_i t} + a_i^{\dagger 2} e^{2i\omega_i t} + a_i a_i^\dagger + a_i^\dagger a_i \right] \quad (4)$$

with $U_1^{(0)} = V^{(0)}\beta$ and $U_2^{(0)} = V^{(0)}\beta^2/8$ where $\beta = 4\sqrt{2}\lambda_i/x_a$ is the ratio between the width λ_i of the motional ground-state probability function of the ion and the position x_a of the atom. Here we have written the position of the ion x_i in the quantized form $x_i = (1/\sqrt{2})\lambda_i \left[a_i e^{-i\omega_i t} + a_i^\dagger e^{i\omega_i t} \right]$, where ω_i is the harmonic trapping frequency, \hat{a}_i^\dagger (\hat{a}_i) represents the creation (annihilation) operator of the 1D harmonic motional quanta (phonon), and $\lambda_i = \sqrt{\frac{\hbar}{m_i\omega_i}}$ with m_i being the mass of the ion. The atom-ion interaction of Eq. (2) changes the potential minimum and phonon frequency of the ion trap. The modified frequency and equilibrium position of the ion trap is given by $\bar{\omega}_i^2 = \omega_i^2 - \frac{8C_4}{m_i x_a^6}$ and $\bar{x} = x_i - \frac{4C_4}{m_i \omega_i^2 x_a^5}$, respectively. Since the trapping frequency of the optical tweezer is much smaller than that of the ion we can assume that the atom does not move much during the time period of gate operation. So we do not consider atomic motion.

A. Phonon blockade

In an ion-atom hybrid quantum system that we consider, phonon blockade manifests through the ion-phonon interaction mediated by atom-ion coupling. When the effective detuning for the ionic motional sideband transitions exceeds the phonon-ionic qubit coupling strength, the transitions between phonon number states becomes off-resonant. Consequently, the emission or absorption of a phonon is suppressed. As a result, a blockade in the transition between the two ionic qubit states will occur.

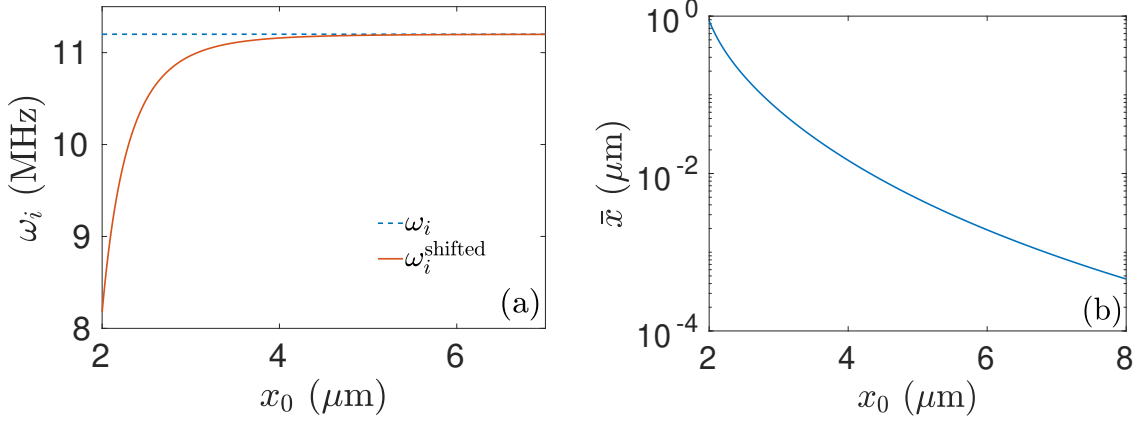


FIG. 2. The shifted phonon frequency (in MHz) (a) and the shifted equilibrium position (in μm)(b) are plotted as a function of ion-atom distance x_0 (in μm) for $^{87}\text{Rb}+^9\text{Be}^+$ system, when the atom is excited to the Rydberg state with principal quantum number $n = 90$. The ion's unperturbed trapping frequency (dashed line) is $2\pi \times 11.2$ MHz.

To realize the phonon blockade and quantum gates, consider that the qubit state $|0\rangle$ of the atom is coupled to the Rydberg state $|r\rangle$ by a two-photon laser pulse. The Hamiltonian describing the system is given by $\hat{H} = \hat{H}_i + \hat{H}_a + \hat{U}_{ia}$ where

$$\hat{H}_i = \frac{\hbar\omega_{01}\sigma_z}{2} + \hat{H}^{(m)} + \hat{H}_L^{(i)}, \quad (5)$$

$$\hat{H}^{(m)} = -\frac{\hbar^2}{2m_i} \frac{d^2}{dx_i^2} + \frac{1}{2}m_i\omega_i^2 x_i^2 \quad (6)$$

describes COM motional dynamics of the ion and ω_{01} is the ionic qubit transition frequency. Here

$$\hat{H}_L^{(i)} = \frac{1}{2}\hbar\Omega_i(\sigma_+ + \sigma_-) \times [e^{i(kx_i - \omega t + \phi)} + e^{-i(kx_i - \omega t + \phi)}] \quad (7)$$

is the interaction of the ionic qubit with the laser, with $\omega = \omega_{L_1} - \omega_{L_2}$ being the difference between the frequencies of the two lasers that couple the two ionic qubit states.

We take the two hyperfine states $|0\rangle_i$ and $|1\rangle_i$ to be the qubit states of the ion. So we can represent $\sigma_+ \equiv |1\rangle_i\langle 0|$ and $\sigma_- \equiv |0\rangle_i\langle 1|$. Ω_i is the Rabi frequency for transition $|0\rangle_i \leftrightarrow |1\rangle_i$. Here the atomic Hamiltonian is

$$\hat{H}_a = \hat{H}_0^{(a)} + \hat{H}_L^{(a)} \quad (8)$$

where

$$\begin{aligned}\hat{H}_0^{(a)} &= -\hbar\delta_a|r_a\rangle\langle r_a| \otimes \mathbb{I}_i \\ \hat{H}_L^{(a)} &= \frac{1}{2}\hbar[\Omega_a|r\rangle_a\langle 0| + \text{H.c.}] \otimes \mathbb{I}_i\end{aligned}\quad (9)$$

where $\mathbb{I}_i = |0\rangle_i\langle 0| + |1\rangle_i\langle 1|$. Here $\hat{U}_{ia} = \hat{U}_1 + \hat{U}_2$ is the ion-atom interaction Hamiltonian. $\hat{H}_L^{(a)}$ is the Hamiltonian that describes interaction of the atomic qubit with lasers and $\delta_a = \delta_r - \frac{V_0}{\hbar}$, $\delta_r = \omega_{\text{sum}} - \omega_{ra}$ with ω_{sum} being the sum of the frequencies of the two lasers that couple the state $|0\rangle$ with $|r\rangle$ and ω_{ra} is the atomic frequency for $|0\rangle \leftrightarrow |r\rangle$ transition. Here Ω_a is the two-photon Rabi frequency for transition $|0\rangle \leftrightarrow |r\rangle$. \hat{U}_{ia} is the ion-atom interaction Hamiltonian.

The unitary operator for the atomic part of the Hamiltonian is

$$\begin{aligned}U_a^{(1)}(t) &= e^{-i\int_0^t (\hat{H}_0^{(a)} + \hat{H}_L^{(a)} + \hat{U}_{ia}(t')) dt' / \hbar} \\ &= e^{-i(\eta(t)\sigma_0^a + \Omega_a t \sigma_x^a + \eta(t)\sigma_z^a) / 2} \\ &= e^{-i\eta(t)\sigma_0^a} \left[\cos \frac{\hat{\theta}}{2} \mathbb{I} - i \frac{\hat{\eta}(t)}{|\hat{\theta}|} \sin \frac{\hat{\theta}}{2} \sigma_z^a - i \frac{\Omega_a t}{|\hat{\theta}|} \sin \frac{\hat{\theta}}{2} \sigma_x^a \right]\end{aligned}\quad (10)$$

Let the initial state be $|000\rangle$ where the atomic, ionic and phononic states are written, respectively. Then, on application of the two-photon laser pulse on the atom for a duration of t , the atom-ion-phonon joint state will be evolved to

$$|\psi(t)\rangle = e^{-i\eta(t)\sigma_0^a} \left[\cos \frac{\hat{\theta}}{2} |000\rangle - i \frac{\hat{\eta}(t)}{|\hat{\theta}|} \sin \frac{\hat{\theta}}{2} |000\rangle - i \frac{\Omega_a t}{|\hat{\theta}|} \sin \frac{\hat{\theta}}{2} |r00\rangle \right]\quad (11)$$

where $|\hat{\theta}| = \sqrt{|\hat{\eta}|^2 + |\Omega_a|^2 t^2}$ and $\hat{\eta}(t) = \int_0^t (\delta_a - \hat{U}_1(t') - \hat{U}_2(t')) dt'$. If we want to make the transition $|0\rangle_a \rightarrow |r\rangle_a$ we have to consider $\Omega_a \gg U_1^{(0)}$ as $\hat{\eta}_{\text{max}} \propto U_1^{(0)}$ such that $\frac{\Omega_a t}{|\hat{\theta}|} \approx \left(1 - \frac{\hat{\eta}^2}{2\Omega_a^2 t^2}\right) \approx 1$ and $\frac{\hat{\eta}}{|\hat{\theta}|} \approx \frac{\hat{\eta}}{\Omega_a t} \left(1 - \frac{\hat{\eta}^2}{2\Omega_a^2 t^2}\right) \ll 1$. Otherwise due to high ion-atom interaction potential higher phonon states would be coupled, so the probability for Rydberg excitation would be reduced. We transform the ionic Hamiltonian into interaction picture under rotating wave approximation [29] in Lamb-Dicke regime

$$H_{int} = \frac{1}{2}\hbar\Omega_i\sigma_+ \{1 + i\eta (ae^{-i\omega_i t} + a^\dagger e^{i\omega_i t})\} e^{i(\phi - \delta_i t)} + \text{H.c.}\quad (12)$$

Lamb-Dicke parameter $\eta = kx_0$, $x_0 = \sqrt{\hbar/2m_i\omega_i}$ is the length scale and ω_i is the trapping frequency of ion. Here $\delta_i = \omega - \omega_{01}$. Now if we take $\delta_i = -\omega_i$ the Hamiltonian is first red sideband resonant, so the Hamiltonian becomes

$$\hat{H}_i = \frac{1}{2}\hbar\Omega_i\eta [a_i\sigma_+ e^{i\phi} + \text{h.c.}]\quad (13)$$

where ϕ is a constant phase. Now if, the atom is in state $|1\rangle$, the red sideband resonance in ion holds good, and ion-phonon transition will occur as a result. Now, if the atom is in Rydberg state, the shifts in the ionic equilibrium position and phonon frequency are large because the ion-atom interaction term increases as n^7 where n is the principal quantum number of Rydberg state. When the shifted phononic frequency is $\bar{\omega}_i = \omega_i - \Delta$, Δ is the frequency shift, the ionic Hamiltonian becomes

$$\hat{H}_i = \frac{1}{2}\hbar\Omega_i\eta [a_i\sigma_+e^{i(\phi+\Delta)t} + \text{h.c.}] \quad (14)$$

This Hamiltonian can be written in time-independent form using a frame transformation. Then the effective Hamiltonian is

$$\hat{H}_i^{eff} = \frac{1}{2}\hbar\Omega_i\eta\sqrt{n}\sigma_x + \frac{\hbar\Delta}{2}\sigma_z \quad (15)$$

As we consider first red sideband coupling, we use only two ion-phonon states which are $|0_i, n\rangle$ and $|1_i, n-1\rangle$, where n is the phonon number. The unitary operator for this effective Hamiltonian is

$$\hat{U}_i = \cos\frac{\theta_i}{2}\mathbb{I} - i\frac{\Delta}{\sqrt{\Omega_n^2 + \Delta^2}}\sin\frac{\theta_i}{2}\sigma_z - i\frac{\Omega_n}{\sqrt{\Omega_n^2 + \Delta^2}}\sin\frac{\theta_i}{2}\sigma_x \quad (16)$$

where $\Omega_n = \Omega_i\eta\sqrt{n}$, $\theta_i = t\sqrt{\Omega_n^2 + \Delta^2}$. Equation (16) shows that if $|\Delta| \gg \Omega_n$ transition between the levels is highly suppressed.

B. Ion-atom two-qubit gate protocol based on phonon blockade

We use this phonon blockade to realize CNOT gate operation. CNOT gate implements the transformation

$$\{|00\rangle, |01\rangle, |10\rangle, |11\rangle\} \rightarrow \{|00\rangle, |01\rangle, |11\rangle, |10\rangle\} \quad (17)$$

where the atom acts as control and the ion as target. Our proposed gate protocol is composed of three consecutive pulses, first pulse is to excite control qubit to a Rydberg state depending on the initial atomic qubit state, second pulse is to excite target qubit conditioned on the control state and third pulse is to deexcite the control qubit if it is in Rydberg state. Here gate protocol is discussed step by step:

Step I: the application of the first π pulse on the control qubit is governed by the Hamiltonian $\hat{H}_1 =$

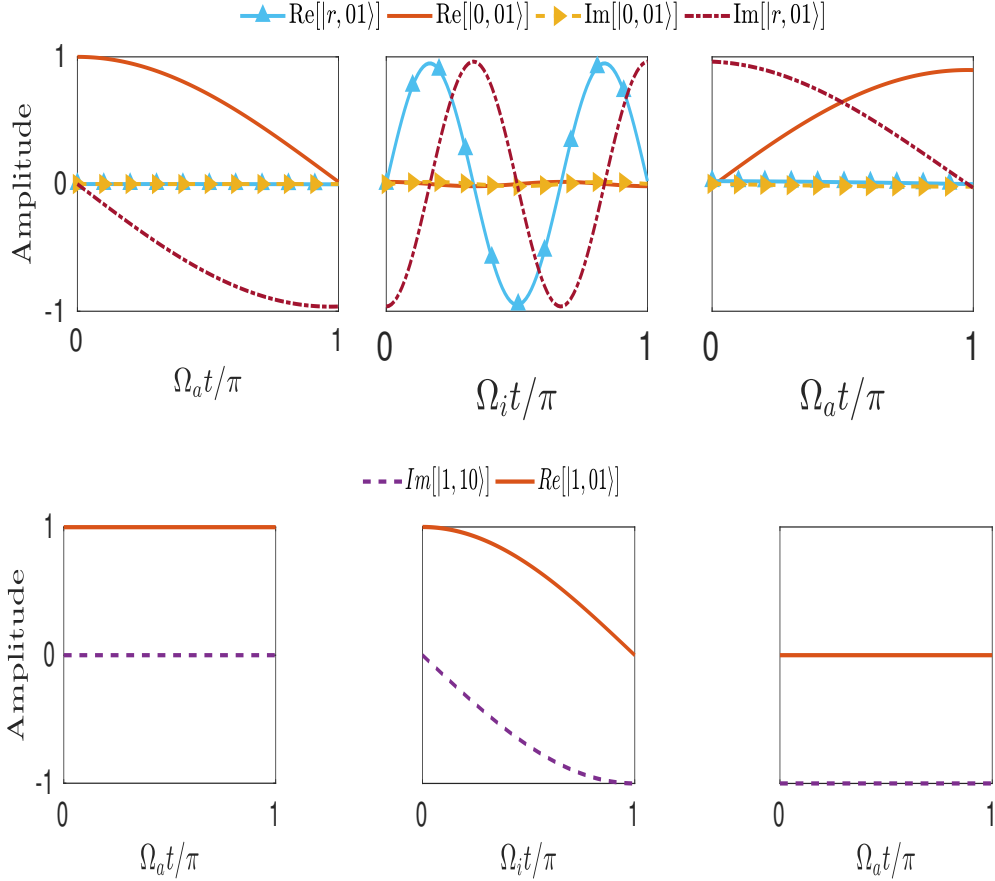


FIG. 3. The real and imaginary parts of the amplitude of different states $|a, ip\rangle$ are plotted as a function of dimensionless time.

\hat{H}_a . For different initial state preparations, one should ideally observe the following evolution after the first π pulse.

$$|0, 01\rangle \rightarrow -i|r, 01\rangle, |0, 10\rangle \rightarrow -i|r, 10\rangle, |1, 01\rangle \rightarrow |1, 01\rangle, |1, 10\rangle \rightarrow |1, 10\rangle \quad (18)$$

We define $|a, ip\rangle \equiv |i\rangle \otimes |a\rangle \otimes |ph\rangle$ where $|a\rangle$, $|i\rangle$ and $|ph\rangle$ define atom, ion and phonon basis, respectively.

Step II: The atomic state does not change during second pulse but it can acquire a phase. The Hamiltonian for second pulse is $\hat{H}_2 = \hat{H}_i$. This pulse is applied for a duration of π/Ω_i . After which the states $-i|r, 01\rangle$, $-i|r, 10\rangle$, $|1, 01\rangle$ and $|1, 10\rangle$ should ideally evolve to $-ie^{i\phi}|r, 01\rangle$, $-ie^{i\phi}|r, 10\rangle$, $-i|1, 10\rangle$ and $-i|1, 01\rangle$, respectively.

Step III: The Rydberg atom is deexcited to the ground state $|0\rangle$ by the application of a pulse

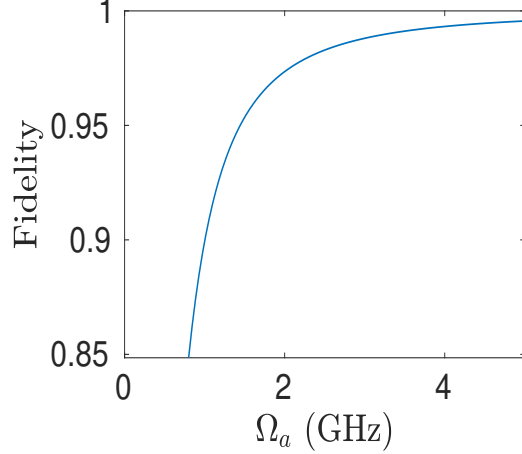


FIG. 4. Fidelity is plotted as a function of the atomic Rabi frequency Ω_a in GHz.

for duration π/Ω_a . So the final states should become $|0, 01\rangle$, $|0, 10\rangle$, $-i|1, 10\rangle$ and $-i|1, 01\rangle$, for a particular ion-atom distance and particular Ω and $\phi = \pi$. Now if a single qubit phase gate, $\hat{S} = \begin{pmatrix} 1 & 0 \\ 0 & i \end{pmatrix}$ is applied on control we get the final states $|0, 01\rangle$, $|0, 10\rangle$, $|1, 10\rangle$ and $|1, 01\rangle$. Thus one can realize an ion-atom CNOT gate.

III. RESULTS AND DISCUSSIONS

For numerical illustration, we consider $^{87}\text{Rb}+^9\text{Be}^+$ system. The atomic qubit is encoded in two hyperfine ground states, $|0\rangle \equiv |n = 5, L = 0, F = 1\rangle$ and $|1\rangle \equiv |n = 5, L = 0, F = 2\rangle$, while an auxiliary Rydberg state $|r\rangle \equiv |n = 90, L = 0, F = 2\rangle$ is used to mediate conditional dynamics. The chosen Rydberg level has a lifetime approximately $100 \mu\text{s}$, which provides sufficiently long coherence window for gate operations with nanosecond to microsecond scale pulses [19]. For this highly excited Rydberg state, the ion-atom interaction is significantly enhanced. The corresponding long-range interaction coefficient C_4 is $5.07 \times 10^{10} C_4^0$ [30] where $C_4^0 = -160 a.u.$. This large enhancement originates from the strong polarizability of the Rydberg atom, scaling as n^7 , and ensures that even at separations of several microns, the ion's motion is strongly influenced when the atom is excited to $|r\rangle$. For the ion, the qubit states are two hyperfine ground states, $|0\rangle \equiv |n = 2, F = 2\rangle$ and $|1\rangle \equiv |n = 2, F = 1\rangle$ [31].

In Fig. 2 we have plotted the shifted and unperturbed phonon frequencies and the shifted equilibrium position as a function of atom-ion distance. We consider that the ion-atom distance is

$2.57\mu\text{m}$ along the x -axis. At this distance, the phonon frequency of the ion's x -axis is shifted to $2\pi \times 10.61$ MHz which is smaller than the harmonic frequency of unperturbed oscillation, which is $2\pi \times 11.2$ MHz, as shown in Fig. 2, but much larger than the linewidth of the ionic state. The unperturbed frequencies of the ion are $2\pi(11.2, 18.2, 29.8)$ MHz, where frequencies in y and z direction are much higher than x -axis frequency [29]. This shift is sufficient to drive the system out of resonance with the first red sideband, thereby blocking the ion's motional transition.

We carry out our numerical work in the Lamb-Dicke regime, with $\eta = 0.1$, such that the ion-phonon coupling remains in the perturbative regime while retaining sensitivity to shifts in trap frequency. We have set the Rabi frequencies for the transition $|0_a\rangle \rightarrow |r_a\rangle$ for the atom is $\Omega_a = 2\pi \times 1$ GHz and the Rabi frequency for ion is $\Omega_i = 2\pi \times 1$ MHz leading to an effective sideband coupling of $\eta\Omega_i = 2\pi \times 0.1$ MHz. Detuning is chosen such that $\delta_r - \frac{1}{\hbar}V_0 = 0$.

The dynamics of the system under the three pulse sequence is illustrated in Fig. 3 which shows the time evolution of the probability amplitudes of different states. When the state is initially prepared in $|0, 01\rangle$, it evolves to $-i|r, 01\rangle$ upon π pulse on the atom. Now, as the atom is excited to $|r, 01\rangle$ state, ion's phononic frequency changes. As a result, the transition between ionic states is blocked but $-i|r, 01\rangle$ oscillates and acquires a phase when a π pulse is applied on the ion. On application of a further π pulse on the atom, the evolved state returns to its initial state provided the phase acquired previously is π . On the other hand, if the system is prepared in $|1, 01\rangle$ state, it is not influenced by the first π pulse as state $|1\rangle_a$ is not coupled to $|r\rangle_a$ as can be seen from Fig. 4. The state goes to $|1, 10\rangle$ on application of second pulse as phonon frequency remains unchanged. Now when the third pulse is applied on the system it is not affected. As a result the final states transform into $|0, 01\rangle$, $|0, 10\rangle$, $-i|1, 10\rangle$ and $-i|1, 01\rangle$ from the initial states $|0, 01\rangle$, $|0, 10\rangle$, $|1, 01\rangle$ and $|1, 10\rangle$, respectively. Now, we apply a **S**-gate, a single qubit phase gate on qubit $|1_a\rangle$. We can thus realize CNOT gate. We calculate the gate fidelity to be 89.94%.

Figure 4 shows the dependence of fidelity on the Rabi frequency of the atom. From this figure, it is worth noting that the fidelity above 90% can be achieved provided that $\Omega_a/2\pi > 1$ GHz. Though it is tough to make Rabi frequency to GHz order but the recent experiment by Huber *et. al.* [32] shows that it is achievable in the case of Rydberg excitation. Higher Rabi frequencies in the GHz regime may couple multiple nearby Rydberg sub-levels [33], in such a case one has to consider a group of Rydberg sub-levels and their net effect on the ion-atom interaction potential. The bottom line is that the ion-Rydberg atom interaction should be sufficiently strong as to cause significant shift in the ionic oscillation frequency, yet remaining in the harmonic oscillation regime.

IV. CONCLUSIONS AND OUTLOOK

In this work, we have proposed and analyzed a hybrid atom-ion two-qubit quantum gate based on a Rydberg induced phonon blockade mechanism. By exploiting the long-range interaction between trapped ion and nearby Rydberg-excited neutral atom, we have demonstrated that the ion's motional sideband transitions can be conditionally suppressed or enabled depending on the internal state of the atom. This work establishes that the state-dependent control of ion-phonon coupling provides a route to implement CNOT gate between atomic and ionic qubits.

A configuration of a linear chain of a few ions in a Paul trap and a few atoms in optical tweezers placed near each ion can serve as a node for distributed quantum computing. Different nodes can be connected by shuttling optical tweezers and thereby transferring and distributing quantum information among different nodes. In such a hybrid quantum architecture, one can use the best features of both charged and neutral qubits at one's disposal. Currently, ion-atom hybrid quantum technology is at its nascent stage, the biggest challenge in the hard-ware front is to place optical tweezers carrying single atoms near an ion so that the trapped ions and atoms form a stable configuration. Once such an architecture is made, addressing ionic and atomic qubits with tailor-made laser pulses for implementing multi-qubit quantum gates or quantum logic is not a problem. In this context, it is worthwhile to note that atomic and ionic qubits will respond to widely different laser frequencies. Another future direction would be to use such a distributed quantum computer as a node for quantum network by entangling the ionic qubits with photonic ones [34].

-
- [1] L. Frunzio, A. Wallraff, D. Schuster, J. Majer, and R. Schoelkopf, [IEEE transactions on applied superconductivity](#) **15**, 860 (2005).
 - [2] A. Blais, R.-S. Huang, A. Wallraff, S. M. Girvin, and R. J. Schoelkopf, [Phys. Rev. A](#) **69**, 062320 (2004).
 - [3] A. Blais, J. Gambetta, A. Wallraff, D. I. Schuster, S. M. Girvin, M. H. Devoret, and R. J. Schoelkopf, [Phys. Rev. A](#) **75**, 032329 (2007).
 - [4] A. Blais, A. L. Grimsmo, S. M. Girvin, and A. Wallraff, [Rev. Mod. Phys.](#) **93**, 025005 (2021).
 - [5] C. R. Monroe and D. J. Wineland, [Scientific American](#) **299**, 64 (2008).
 - [6] R. Blatt and D. Wineland, [Nature](#) **453**, 1008 (2008).
 - [7] R. Blatt and C. F. Roos, [Nature Physics](#) **8**, 277 (2012).

- [8] C. D. Bruzewicz, J. Chiaverini, R. McConnell, and J. M. Sage, [Appl. Phys. Rev. **6** \(2019\)](#).
- [9] A. Negretti, P. Treutlein, and T. Calarco, [Quantum information processing **10**, 721 \(2011\)](#).
- [10] D. S. Weiss and M. Saffman, [Physics Today **70**, 44 \(2017\)](#).
- [11] L. Henriët, L. Béguin, A. Signoles, T. Lahaye, A. Browaeys, G.-O. Reymond, and C. Jurczak, [Quantum **4**, 327 \(2020\)](#).
- [12] T. Graham, Y. Song, J. Scott, C. Poole, L. Phuttitarn, K. Jooya, P. Eichler, X. Jiang, A. Marra, B. Grinkemeyer, *et al.*, [Nature **604**, 457 \(2022\)](#).
- [13] S. J. Evered, D. Bluvstein, M. Kalinowski, S. Ebadi, T. Manovitz, H. Zhou, S. H. Li, A. A. Geim, T. T. Wang, N. Maskara, H. Levine, G. Semeghini, M. Greiner, V. Vuletić, and M. D. Lukin, [Nature **622**, 268 \(2023\)](#).
- [14] D. Bluvstein, S. J. Evered, A. A. Geim, S. H. Li, H. Zhou, T. Manovitz, S. Ebadi, M. Cain, M. Kalinowski, D. Hangleiter, J. P. Bonilla Ataides, N. Maskara, I. Cong, X. Gao, P. Sales Rodriguez, T. Karolyshyn, G. Semeghini, M. J. Gullans, M. Greiner, V. Vuletić, and M. D. Lukin, [Nature **626**, 58 \(2024\)](#).
- [15] M. Saffman, T. G. Walker, and K. Mølmer, [Rev. Mod. Phys. **82**, 2313 \(2010\)](#).
- [16] L. Isenhower, E. Urban, X. L. Zhang, A. T. Gill, T. Henage, T. A. Johnson, T. G. Walker, and M. Saffman, [Phys. Rev. Lett. **104**, 010503 \(2010\)](#).
- [17] L. Béguin, A. Vernier, R. Chicireanu, T. Lahaye, and A. Browaeys, [Phys. Rev. Lett. **110**, 263201 \(2013\)](#).
- [18] A. Browaeys and T. Lahaye, [Nature Physics **16**, 132 \(2020\)](#).
- [19] K. Wang, C. P. Williams, L. R. Picard, N. Y. Yao, and K.-K. Ni, [PRX Quantum **3**, 030339 \(2022\)](#).
- [20] C. Zhang and M. Tarbutt, [PRX Quantum **3**, 030340 \(2022\)](#).
- [21] S. S. Rej and B. Deb, [arxiv \(2025\)](#), [arXiv:2507.02531 \[quant-ph\]](#).
- [22] S. S. Rej and B. Deb, [New J. Phys. **28**, 014513 \(2026\)](#), [arXiv:2511.04359 \[quant-ph\]](#).
- [23] S. S. Rej, S. Ray, and B. Deb, [arxiv \(2026\)](#), [arXiv:2601.06665 \[quant-ph\]](#).
- [24] N. V. Ewald, T. Feldker, H. Hirzler, H. A. Fürst, and R. Gerritsma, [Phys. Rev. Lett. **122**, 253401 \(2019\)](#).
- [25] T. Secker, N. Ewald, J. Joger, H. Fürst, T. Feldker, and R. Gerritsma, [Phys. Rev. Lett. **118**, 263201 \(2017\)](#).
- [26] M. Tomza, K. Jachymski, R. Gerritsma, A. Negretti, T. Calarco, Z. Idziaszek, and P. S. Julienne, [Rev. Mod. Phys. **91**, 035001 \(2019\)](#).

- [27] S. Mudli, S. Mal, S. S. Rej, A. Dey, and B. Deb, [Phys. Rev. A **110**, 062618 \(2024\)](#).
- [28] M. Mazzanti, C. Robalo Pereira, N. A. Diepeveen, B. Gerritsen, Z. Wu, Z. E. D. Ackerman, L. P. H. Gallagher, A. Safavi-Naini, R. Gerritsma, and R. X. Schüssler, [Phys. Rev. A **110**, 043105 \(2024\)](#).
- [29] D. Leibfried, R. Blatt, C. Monroe, and D. Wineland, [Rev. Mod. Phys. **75**, 281 \(2003\)](#).
- [30] A. A. Kamenski and V. D. Ovsianikov, [J. Phys. B: At. Mol. Opt. Phys. **47**, 095002 \(2014\)](#).
- [31] D. M. Meekhof, C. Monroe, B. E. King, W. M. Itano, and D. J. Wineland, [Phys. Rev. Lett. **76**, 1796 \(1996\)](#).
- [32] B. Huber, T. Baluktsian, M. Schlagmüller, A. Kölle, H. Kübler, R. Löw, and T. Pfau, [Phys. Rev. Lett. **107**, 243001 \(2011\)](#).
- [33] Silpa, S. K. Barik, S. Chaudhuri, and S. Roy, [Opt. Continuum **1**, 1176 \(2022\)](#).
- [34] M. Canteri, Z. X. Koong, J. Bate, A. Winkler, V. Krutyanskiy, and B. P. Lanyon, [Phys. Rev. Lett. **135**, 080801 \(2025\)](#).